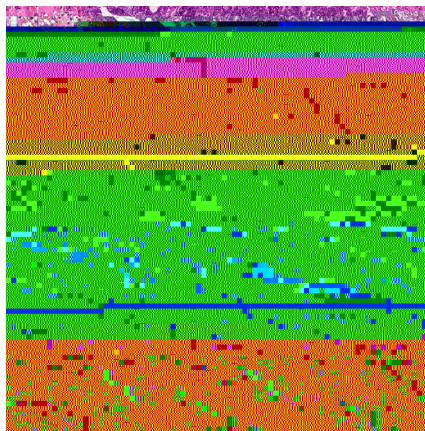
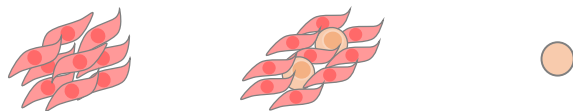

na municat

DNA

P C

G



D. 2). F. Prickle1, DNA
 K R- P C (50-70%)
 MEF (>90%),
 ▲ 2 E C (<10%), 2
 48-51
 F 13
 MEF
 ICR II
 (P_w /A, Peg3, Gnas, Commd1-Zrsr1, Mctc2-H13, Kcqn1-Kcnq1ot1,

Mest/Peg1, Plagl1/Zac1, Grb10, Igf2r Impact)
 (Igf2-H19 Dlk1-Dio3) (F .2A; F .2B;
 D. 2).
 ▲ 2 E C 2
 52,53
 (>75%, <25%,
) K R- P C .
 ICR F K R- P C (F .2A;

(F . 4E; F . 4C). Q
(Dlk1-Dio3 Igf2-H19)
ICR (F . 4B; F . 4E).
Igf2-H19 (F . 4B; F . 4E, F).
H19 (F . 4C). A.

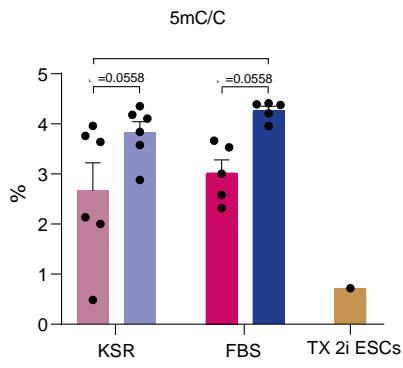
Dlk1-Dio3 4 5
P C (F . 4B). M FB 1 P C
Dlk1-Dio3 ICR Meg3
M FB 5 Meg3
F . 5A). C Meg3

Fig. 2 | Hypomethylation defects in KSR-iPSCs. A Methylome-wide association study (MWAS) of CpG sites in KSR-iPSCs. The y-axis represents the CpG sites, and the x-axis represents the methylation level. The plot shows the distribution of CpG sites across different genomic regions: Dlk1-Dio3, Igf2-H19, P_W/A ICR, MEF, (FK R1-6), (MK R1-6), P_C, 2 E_C; E_D, C_G, C_G, C_G, Peg3. The sample sizes for each region are: Dlk1-Dio3: n = 27; Igf2-H19: n = 16; P_W/A : n = 24; Peg3: n = 24.

13 Dlk1-Dio3 (F . 5A) F . 5A,B; D . 2). Meg3
 Meg3 Dlk1-Dio3 ICR (F . 5B).
 DNA K R FB

I J. 0

K R- FB - P C .
 F 5- (5 C) L
 C (LC-M /M)
 K R- FB - P C ▲ 2 E C . LC-M
 P C
 5 C P C
 (F 5B).
 E C / P C 5 C
 54,55,57 Q
 5 C K R- FB P C P C
 (F 5B). A
 K R- FB - P C 5 C
 ▲ 2 E C (F 5B), 50,51
 2
 P C DNA
 E C 58
 (IAP),
 R (L R) II (ER)⁵⁹
 L I N E I
 (LINE1), LINE1-A (LI-A) LINE1- (LI-),
 -L R 60 B
 58
 (F 5C). IAP DNA P C
 FB LI-A
 K R- FB - P C (F 5C).
 DNA
 ▲ 2 E C (F 5C) 58 I
 LI- 6 39999961()1.2000000416(15.370000076(-4.1999999())15.39999961(,325..5()19()13.37999992



5hmC/C

■ Females
■ Males
■ TX 2i ESCs

FB (P_W/A)
 O K R
 R H 1
 P C
 (F 5A)
 FB
 EA1 (-/+),

K R FB 1:1

K R FB
FB K R.

Igf2-H19

Dlk1-Dio3 4 6 K R/FB - P C (F 7A). H

(Mcts2-H13, Peg3, Igf2-H19

Commd1-Zrsr1) (F 7A),

(F 9A). D

K R/FB

K R-P C

O C FB

FB + C

Dlk1-Dio3 ICR³⁸

Peg3, P_w /A Commd1-Zrsr1

Prickle1

5' C
DNA
F . 7F). 5' C
Xist,
▲ (F . 6B). 5' C
(F . 7E).

PC.E PC

10%

L MCI70 HD

L DM2500

fl s (F)

C

ID.

M I (MI) MI

R

G 0.5.0 (

1.15.

A

2. Mandai, M. et al. iPSC-derived retina transplants improve vision in rd1 end-stage retinal-degeneration mice. *Stem Cell Res.* **8**, 69–83 (2017).
3. Shi, Y., Inoue, H., Wu, J. C. & Yamanaka, S. Induced pluripotent stem cell technology: a decade of progress. *Nat. Rev. Drug Discov.* **16**, 115–130 (2017).
4. Buganim, Y., Faddah, D. A. & Jaenisch, R. Mechanisms and models of somatic cell reprogramming. *Nat. Rev. Genet.* **14**, 427–439 (2013).
5. Schiebinger, G. et al. Optimal-transport analysis of single-cell gene expression data. *Cell* **170**, 451–464 (2017).

49. Habibi, E. et al. Whole-genome bisulfite sequencing of two distinct interconvertible DNA methylomes of mouse embryonic stem cells. *Cell Stem Cell* **13**, 360–369 (2013).

